J Incl Phenom Macrocycl Chem (2011) 70:187–195
DOI 10.1007/s10847-010-9891-4

ORIGINAL ARTICLE

DNA–interactions of ruthenium(II) & cobalt(III) phenanthroline and bipyridine complexes with a planar aromatic ligand 2-(2-fluronyl)1H-imidazo[4,5-f][1,10-Phenanthroline]

Mynam Shilpa · J. Naveena Lavanya Latha · A. Gayatri Devi · A. Nagarjuna · Yata Praveen Kumar · Penumaka Nagababu · S. Satyanarayana

Received: 21 December 2009 / Accepted: 14 October 2010 / Published online: 27 October 2010

Abstract The ligand 2-(2-fluronyl)1H-imidazo[4,5-f][1,10-Phenanthroline] (fyip) was synthesized and four mixed ligand complexes $[Ru(phen)_2fyip]^{2+}$ **1**, $[Co(phen)_2fyip]^{3+}$ **2**, $[Ru(bpy)_2fyip]^{2+}$ **3** and $[Co(bpy)_2fyip]^{3+}$ **4** are prepared. These complexes are characterized by IR, ^1H, ^{13}C NMR and mass. The interaction of these complexes with calf thymus DNA have been studied. DNA binding was monitored by absorption, fluorescence spectroscopy, viscosity and thermal denaturation studies. All complexes bind to DNA through an intercalative mode with comparable strength and their intrinsic binding constants follows the order **1** > **2** > **3** > **4**. These four complexes promote the photocleavage of plasmid pBR322 DNA upon irradiation at 302 nm. Antibacterial activity of these complexes have also been studied.

Keywords Polypyridyl ligand · Binding affinity · Luminescence · Minimum inhibitory concentrations · Photocleavage

M. Shilpa · A. Gayatri Devi · Y. P. Kumar · P. Nagababu · S. Satyanarayana (✉)
Department of Chemistry, Osmania University, Hyderabad 500007, Andhra Pradesh, India
e-mail: ssnsirasani@gmail.com

J. N. L. Latha
Department of Biotechnology, Krishna University, Machilipatnam, India

A. Nagarjuna
Department of Microbiology, Osmania University, Hyderabad, India

Introduction

The interaction of ruthenium(II) complexes with DNA have attracted attention because of their potential utilities for DNA structure probes, DNA dependent electron transfer probes, DNA-foot printing and sequence-specific cleaving agents [1–4]. Luminescent transition metal complexes such as $Ru(L)_3^{2+}$ (L = 1,10, phenanthroline (or) its substituted derivatives) have been utilized as photo sensitizers in such areas as solar energy conversion [5], electron transfer studies [6, 7] and probes of macromolecular structure [8]. These complexes are the most frequently used probes in the above applications due to strong visible absorption, high photo chemicals stability, efficient luminescence, and relatively long-lived metal to ligand charge transfer (MLCT) excited states [9]. Barton and co-workers have reported some accelerated electron-transfer between metal complexes mediated by DNA [10]. The great success of using Ru–polypyridyl complexes for probing DNA binding is documented in the literature [11–14]. Several polypyridyl cobalt(III) complexes have been reported which bind DNA through intercalation and are effective photo nucleases. Ji and co-workers have published several reports on the DNA binding and photo nuclease activities of cobalt(III) complexes [13, 15–20]. In our previous reports [21, 22], we have synthesized a series of novel polypyridyl type ligands, containing an imidazo ring (L) and demonstrated the binding of $[Co(bpy)_2\ L]^{3+}$ and $[Co(phen)_2\ L]^{3+}$ type complexes to DNA via the intercalation of L into the DNA base pairs. In this work, we have synthesized four complexes. $[M(phen)_2L]$ and $[M\ (bpy)_2L]$ ($M = Ru^{2+}$, Co^{3+}), L = (fyip) 2-(2-fluronyl)1H-imidazo[4,5-f][1,10-Phenanthroline] and the DNA binding properties of complexes studied with electronic absorption, steady-state emission studies, viscosity and thermal

denaturation. These complexes can intercalate into DNA base pairs and cleave the pBR322 DNA with high activity upon irradiation.

Experimental section

Materials and instrumentation

Emission measurements were carried by using a *Elico spectroflurometer* model *SL174*. UV–Visible spectra were recorded on *an Elico Bio-spectrophotometer model BL198.* IR spectra were recorded, in KBr phase on *Perkin–Elmer FTIR-1605.* Es^+-MS mass spectra were recorded on *JEOL SX 102/DA-6000 mass spectrometer/data system*. ^1H and ^{13}C-NMR spectra were measured on a *Varian XL 300 MHz* spectrometer with DMSO-d_6 as a solvent at room temperature and tetramethylsilane (TMS) as the internal standard.

DNA binding experiments

Doubly distilled water was used to prepare tris buffer (5 mM Tris–HCl, 10 mM NaCl pH = 7.1). All chemicals were of reagent grade. A solution of calf thymus DNA in buffer gave a ratio of 1.8–1.9 absorbance at 260 and 280 nm, indicating DNA was free of protein [23]. The DNA concentration per nucleotide was determined by using a molar absorption coefficient (6,600 M^{-1} cm^{-1}) at 260 nm [24].

The absorption titrations of the complex in buffer were performed by titrating fixed concentration of complex (10 μM). Complex–DNA solutions were allowed to incubate for 5 min before recording the absorption spectra. In order to evaluate the binding strength of the complex, the intrinsic binding constant K_b, with CT–DNA was obtained by monitoring the change in the absorbance at metal to ligand charge transfer (MLCT) band, with increasing concentration of DNA. The intrinsic binding constant K_b, was calculated from Eq. 1 [25].

$$[DNA]/(\varepsilon_a - \varepsilon_f) = [DNA]/(\varepsilon_b - \varepsilon_f) + 1/K_b(\varepsilon_b - \varepsilon_f) \quad (1)$$

where [DNA] is the concentration of DNA. ε_a, ε_f and ε_b corresponds to the apparent absorption coefficient A_{obsd}/[complex], the extinction coefficient for the free complex, and the extinction coefficient for the complex in the fully bound form respectively. In plots of $[DNA]/(\varepsilon_a - \varepsilon_f)$ versus [DNA]. K_b is given by the ratio of slope to the intercept.

In the emission studies fixed metal complex concentration (6 μM) was taken varying concentration (0–150 μM) of DNA was added. The excitation wavelength was taken fixed and the emission range was adjusted before measurements. The fraction of the ligand bound was calculated from the relation $C_b = C_t[(F - F_0)/F_{max} - F_0)]$, where C_t is the total complex concentration, F is the observed fluorescence emission intensity at a given DNA concentration, F_0 is the intensity in the absence of DNA, and F_{max} is when complex is fully bound to DNA. Binding constant (K_b) was obtained from a Scatchard plot of r/C_f versus r, where r is the C_b/[DNA] and C_f is the concentration of free complex.

Viscosity experiments were carried out in an Ostwald viscometer maintained at a constant temperature 30.0 ± 0.1 °C in a thermostatic water-bath. Calf thymus DNA samples approximately 200 base pairs were prepared by sonicating in order to minimize complexities arising from DNA flexibility [26]. Flow time was measured with a digital stopwatch and each sample was measured three times, and then an average flow time was calculated. Data were presented as $(\eta/\eta_0)^{1/3}$ versus the [complex]/[DNA], where η is the viscosity of DNA in presence of complex and η_0 is the viscosity of DNA alone. Viscosity values were calculated from the observed flow time of DNA and DNA + complex [27].

Thermal denaturation studies were carried out with an Elico Bio-spectrophotometer model BL198, equipped with a temperature-control programmer (±0.1 °C). Absorbance at 260 nm was continuously monitored with increase in temperature 1 °C per min, for solutions of CT–DNA (100 μM) in the absence and presence of the ruthenium(II) and cobalt(III) complexes (10 μM).The data was presented as OD vs temperature, at 260 nm respectively.

The antibacterial tests were performed by the standard disc diffusion method [28]. The complexes were screened for antibacterial activity against standard microorganisms such as *Staphylococcus aureus*, *E. coli*, *Pseudomonas aeruginosa* and *Klebsiella pneumonia*. The Mueller Hinton agar was prepared and poured fresh into sterile Petri plates and allowed to dry, and inoculate 0.2 mL of bacterial culture which has 10^6 cells/mL concentrations. The complex was dissolved in DMSO to get a final concentration of 100 μL per disc. Each plate contains standard microorganisms with four different complexes (5 μL each compound) and standard antibiotics such as ampicillin, cotrimaxizole and norfloxacin were also tested on these standard microorganisms as controls, and kept in the refrigerator for 5 min and these were transferred to the incubator at 37 °C. After 24 h of incubation, the zone of inhibition of the complexes as well as standard antibiotics on standard microorganisms were checked. The minimum inhibitory concentrations (MICs) for these complexes were measured.

For the gel electrophoresis experiments, Supercoiled pBR322 DNA (0.2 μM) was treated with Ru(II) complexes and the samples were then irradiated at room temperature with a UV lamp 302 nm for ½ h. Samples were analyzed

by electrophoresis for 2.5 h at 40 V on a 0.8% agarose gel in Tris–acetic acid–EDTA buffer. The gel was stained with 1 μg/mL ethidium bromide and then photographed under UV light (Fig. 1).

Synthesis

The compounds 1,10, phenanthroline-5,6-dione [29], *cis*-$[Ru(phen)_2Cl_2]\cdot 2H_2O$ and *cis*-$[Ru(bpy)_2Cl_2]\cdot 2H_2O$ [30], *cis*-$[Co(phen)_2Br_2]Br\cdot 2H_2O$ and *cis*-$[Co(bpy)_2Br_2]Br\cdot 2H_2O$[31] were synthesized according to the procedure available in literature.

Synthesis of (fyip) 2-(2-fluronyl)1-H-imidazo[4,5-f][1,10-Phenanthroline]

The ligand was synthesized according to the procedure in the literature [32]. A mixture of phen–dione (0.53 g, 2.50 mmol), 2-fluorene carboxaladehyde (0.679, 3.50 mmol) ammonium acetate (3.88 g, 50.0 mmol) and glacial acetic acid (15 mL) was refluxed together for 4 h. The above solution was cooled to room temperature and diluted with water. Drop wise addition of conc. aq. NH_3 gave a dark orange ppt, which was collected washed with H_2O and dried, the crude product thus obtained was purified by recrystallization with ethanol and dried (80%). The ES^+-MS spectrum shows a molecular ion peak at *m/z* 385 which is equivalent to its molecular weight (calc.: 384).

*Synthesis of $[Ru(phen)_2fyip](ClO_4)_2\cdot 3H_2O$ (**1**)*

A mixture of *cis*-$[Ru(phen)_2Cl_2]\cdot 2H_2O$ (0.12 g, 0.16 mmol), fyip (0.061 g, 0.16 mmol) and methanol/water 1:1 (15 mL) was refluxed for about 5 h. It was then cooled to room temperature. After filtration an equal volume of saturated aqueous sodium per chlorate solution was added. The brownish solid was collected and washed with small amount of water, ethanol then dried under vacuum (72%). ES^+-MS: calculated: 1024, found: 1026.

*Synthesis of $[Ru(bpy)_2fyip](ClO_4)_2\cdot 1.5\ H_2O$ (**2**)*

This red complex was synthesized as above, with *cis*-$[Ru(bpy)_2Cl_2]\cdot 2H_2O$ (0.10 g, 0.016 mmol) in place of *cis*-$[Ru(phen)_2Cl_2]\cdot 2H_2O$ (68%). ES^+-MS: calculated: 1041, found: 1041.

*Synthesis of $[Co(phen)_2fyip](ClO_4)_3$ (**3**)*

This complex was prepared by mixing *cis*-$[Co(phen)_2Br_2]$-$Br\cdot 2H_2O$ (0.716 g, 1.0 mmol) and fyip (0.576 g, 1.5 mmol) in 20 mL of ethanol and was refluxed for 6 h. After filtration it was then cooled to room temperature, and saturated ethanolic solution of sodium perchlorate was added. The light yellowish solid was collected and washed with small amount of water and then dried under vacuum (66%).

*Synthesis of $[Co(bpy)_2fyip](ClO_4)_3$ (**4**)*

This complex was synthesized according to the procedure given above. *cis*-$[Co(bpy)_2Br_2]Br\cdot 2H_2O$ (0.578 g, 1.0 mmol) and fyip (0.576 g, 1.5 mmol) taken in 20 mL of ethanol refluxed for 5 h. Yellow color solid obtained (66%).

These complexes were characterized by IR, ^1H and ^{13}C NMR and the data are given in Tables 1, 2.

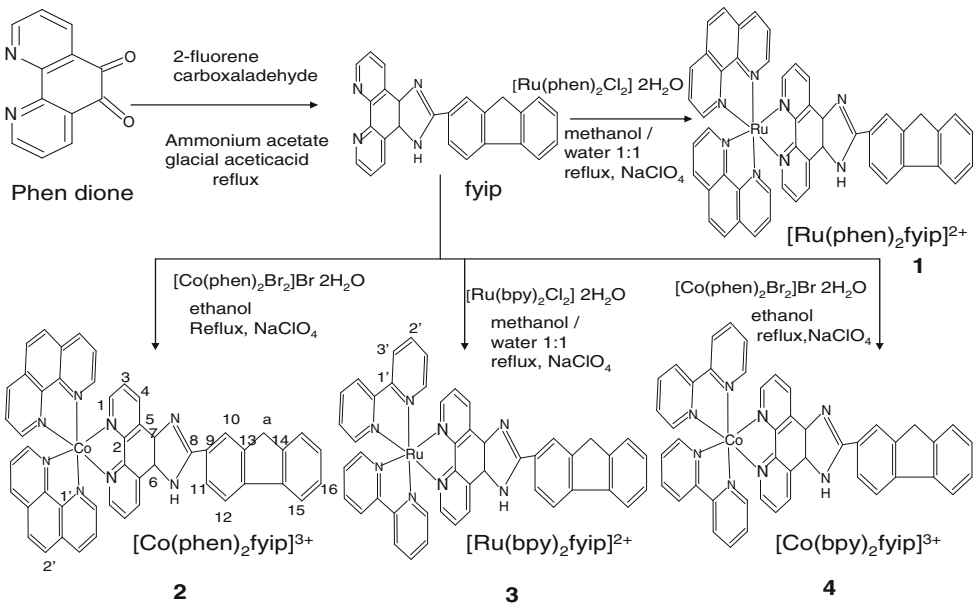

Fig. 1 Synthetic routines of the Ru(II) and Co(III) complexes

Table 1 ^{1}H NMR and IR data of complexes

Complexes	IR-data				^{1}H-NMR (300 MHz, DMSO-d_6, TMS)
	C=C	C=N	M–N(phen)/bpy	M–L	
Fyip					9.1 (d, 2H), 8.9 (d, 2H), 8.5 (s, 1H), 8.3 (d, 1H), 8.0 (d, 1H), 7.8 (d, 2H), 7.5 (d, 2H), 7.20 (d, 2H), 3.95 (CH_2 of ligand, 2H)
[Ru(phen)$_2$fyip]	1,410	1,540	610	705	9.1 (d, 6H), 8.8 (d, 6H), 8.4 (s, 1H), 8.2 (d, 1H), 8.0 (d, 1H), 7.7 (d, 2H), 7.4 (m, 6H) 7.2 (d, 2H), 7.1 (s, 4H) 4.1 (s, 2H)
[Co(phen)$_2$fyip]	1,440	1,570	605	730	9.5 (d, 6H), 9.2 (d, 6H), 8.5 (d, 1H), 8.3 (d, 1H), 8.2 (d, 4H), 8.0 (d, 2H), 7.7 (s, 1H), 7.6 (d, 1H), 7.5 (t, 6H), 4.1 (CH_2 of ligand, 2H)
[Ru(bpy)$_2$fyip]	1,420	1,560	623	712	9.3 (d, 2H), 9.1 (d, 4H), 8.9 (d, 4H), 8.6 (s, 1H), 8.4 (d, 2H), 8.2 (d, 2H), 8.0 (t, 4H), 7.9 (d, 2H), 7.7 (t, 2H), 7.4 (t, 4H), 4.2 (CH_2 of ligand, 2H)
[Co(bpy)$_2$fyip]	1,470	1,600	625	690	9.4 (d, 2H), 9.17 (d, 4H), 8.7 (d, 4H), 8.4 (d, 2H), 8.10 (s, 1H), 7.95 (d, 2H), 7.7 (d, 3H), 7.65 (d, 3H), 7.35 (t, 2H), 7.21 (d, 4H), 3.9 (CH_2 of ligand, 2H)

Table 2 ^{13}C [^{1}H] NMR data of complexes

[Ru(phen)$_2$fyip]	[Co(phen)$_2$fyip]	[Ru(bpy)$_2$fyip]	[Co(bpy)$_2$fyip]
153.04(C_1)	153.57(C_1)	156.81(C_1, C_5)	156.77(C_1)
152.67(C_2, C_8)	150.83(C_2, C_8)	121.89(C_2, $C_{3'}$)	123.11(C_2)
123.7(C_3)	123.42(C_3, C_{16})	136.43(C_3)	137.79(C_3, $C_{2'}$)
143.76(C_4, C_9)	140.14(C_4)	127.81(C_4, C_{12})	126.58(C_4, C_7)
128.0(C_5, C_{10})	129.24(C_5, C_7)	130.47(C_6, C_7)	152.96(C_5)
140.24(C_6)	131.85(C_6)	151.53(C_8)	127.58(C_9, C_6)
136.76(C_7)	135.70(C_9)	133.64(C_9)	151.56(C_8)
127.69(C_{11})	126.96(C_{10})	126.28(C_{10})	125.91(C_{10}, $C_{3'}$)
130.42(C_{12})	127.58(C_{11})	124.41(C_{11}, C_{15})	123.11(C_{11}, C_{15})
147.19(C_{13}, C_{14})	128.70(C_{12})	143.41(C_{13}, $C_{1'}$)	124.40(C_{12}, C_{16})
126.89(C_{15})	143.75(C_{13}, $C_{1a'}$)	137.96(C_{14})	144.87(C_{13})
125.51(C_{16}, $C_{2'}$)	141.88(C_{14})	122.16(C_{16})	140.21(C_{14})
150.11($C_{1'}$)	125.85(C_{15}, $C_{2'}$)	135.65($C_{2'}$)	149.82($C_{1'}$)
36.42(CH_2 group)	36.31(CH_2 group)	37.42(CH_2 group)	130.56($C_{2'}$)
			36.44(CH_2 group)

Results and discussion

Electronic absorption titration

Electronic absorption spectroscopy technique is utilized to determine the binding of complexes with the DNA helix. A complex bound to DNA through intercalation is characterized by the change in absorption (hypochromism) and red shift in wave length due to a strong stacking interaction between the aromatic chromophore and the DNA base pairs. The extent of hypochromism is consistent with the strength of the intercalative interaction [33–35]. The electronic absorption spectra of the polypyridyl ruthenium(II) complex [Ru(phen)$_2$fyip]$^{2+}$ in the absence and the presence of CT–DNA in tris buffer (pH = 7.2) are given in Fig. 2. Upon the addition of CT–DNA, the electronic absorptions of **1**, **2**, **3** and **4** experienced significant hypochromism (H%) and red-shift are given in Table 3. These data imply that these complexes bind to DNA in an intercalation mode [36, 37]. The absorption spectrum of all four complexes are characterized by distinct and intense MLCT transitions in the visible region which are attributed to Ru(dπ) $\rightarrow$ bipy(π^*) and phen π^* and Ru dπ $\rightarrow$ fyip. The bands below 350 nm are attributed to intra ligand (IL) $\pi \rightarrow \pi^*$ transitions while the metal to ligand charge transfer MLCT bands appear at lower energy (470 nm).

In order to compare the binding strengths of these complexes, the intrinsic binding constants K_b of the four complexes with CT–DNA were obtained by monitoring the changes in absorbance at 453, 320, 463 and 310 nm respectively for **1**, **2**, **3** and **4** complexes. The value of K_b was evaluated using Eq. 1 [25]. Intrinsic binding constants K_b, of the four complexes, are given in Table 3. These data confirm that these complexes bind to DNA in the order

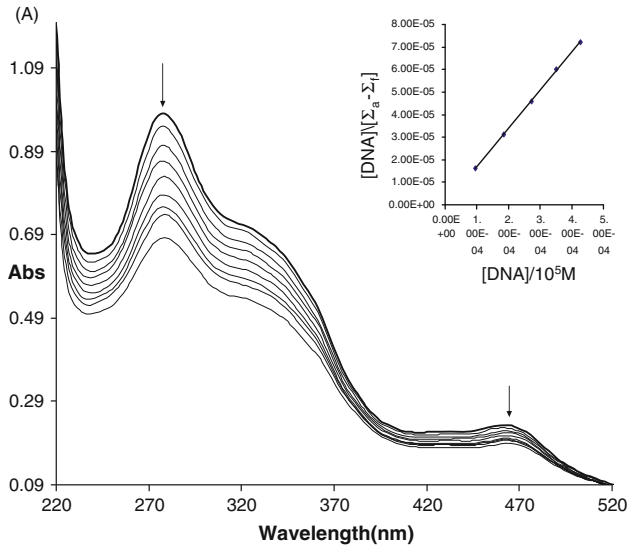

Fig. 2 Absorption spectra of $[Ru(phen)_2fyip]^{2+}$ in tris-buffer upon addition of CT–DNA in absence (*top*) and presence of CT–DNA (*lower*) the [complex] = 10–15 μm; [DNA] = 0–126 μm. *Insert* plots of [DNA]/($\varepsilon_a - \varepsilon_f$) versus [DNA] for the titration of DNA with complex. *Arrow* shows change in absorption with increasing DNA concentration

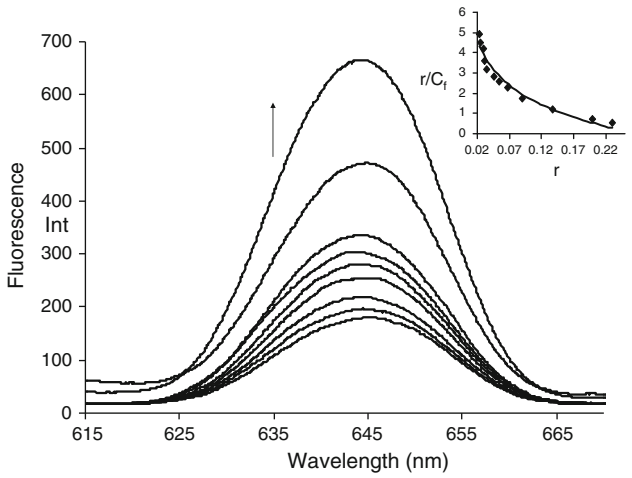

Fig. 3 Fluorescence emission spectra of complex $[Co(phen)_2fyip]^{3+}$ tris-buffer (pH = 7.0) in the presence of CT–DNA [complex] = 10 μM. The *arrow* shows the fluorescence intensity change upon increase of DNA concentration. *Inset* is the binding isotherm for the interaction of complex $[Co(phen)_2fyip]^{3+}$ with DNA. The *line* is the best fit, obtained by nonlinear least-square analysis to the simple McGhee–Von Hippel model

1 > 2 > 3 > 4. The binding constant depends on the planarity of the intercalating ligand. Since the intercalator is same in all the four complexes the difference in K_b depends on the ancillary ligand and metal. The ancillary ligand phenanthroline compared to bipy is more planar and hydrophobic, hence the binding affinity is more for complex **1** and **2**. We know that Ru^{2+} complexes binds to DNA much stronger than Co^{3+} complexes. Since the size of ruthenium metal is higher than cobalt and the difference in self aggregation and electronic effect induced by the ruthenium metal is also higher. Ru^{2+} has 4d orbital which will delocalize more than 3d (Co^{3+}). This makes the intercalating ligand electron deficient in Ru(II) complexes than Co(III) and hence Ru(II) complexes binds strongly than Co(III).

Steady-state emission studies

In the absence of DNA, complex can exhibit luminescence in tris- buffer at ambient temperature. The excitation peaks appeared at 467, 343, 467, 382 nm and the emission appeared at 599, 421, 604, 447 nm for **1**, **2**, **3** and **4** complexes, respectively. Upon addition of CT–DNA, the emission intensities of complex **1**, **2**, **3** and **4** increase around 4.95, 2.82, 2.00 and 1.69 times than the complex alone in Fig. 3. This implies that complexes can strongly interact with DNA and be protected by DNA efficiently, since the hydrophobic environments inside the DNA helix reduces the accessibility of solvent water molecules to the complex and the complex mobility is restricted at the binding site, leading to decrease of the vibrational modes of relaxation, and hence fluorescence intensity increases. Binding data were cast into the form of Scatchard plot of r/C_f versus r, where r is the binding ratio C_b/[DNA] and C_f is the free ligand concentration. The binding constants calculated from Fig. 3 (9.5×10^5) are comparable with absorption data. The K values are given in Table 3.

Emission quenching experiments using $[Fe(CN)_6]^{4-}$ as quencher were studied to observe the binding of the complexes with CT–DNA. The Stern–Volmer quenching constant K_{sv} can be determined by using Stern–Volmer equation [38].

Table 3 Comparison of DNA-binding data of complexes

Complexes	Hypochromism (%)	Absorption Δ_λ	Absorption binding constant K_b	Emission binding constant	(K_{sv})		
					Only com	1:30	1:200
$[Ru(phen)_2fyip]^{2+}$	13.3	13	1.8×10^6	5.2×10^6	1053.2	425.3	71.0
$[Co(phen)_2fyip]^{3+}$	10.4	6	9.2×10^5	9.7×10^5	830.6	211.5	28.2
$[Ru(bpy)_2fyip]^{2+}$	9.9	5	8.05×10^5	8.62×10^5	525.5	145.7	17.2
$[Co(bpy)_2fyip]^{3+}$	7.3	3	1.8×10^5	2.8×10^5	307.9	125.2	7.19

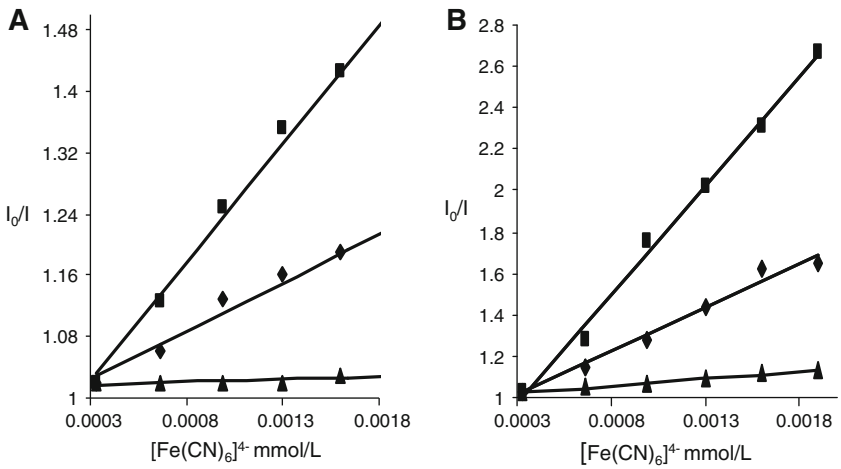

Fig. 4 Emission quenching of complexes **A** $[Co(bpy)_2fyip]^{3+}$ and **B** $[Ru(phen)_2fyip]^{2+}$] with $[Fe(CN)_6]^{4-}$ in the absence of DNA (*filled square*), presence of DNA 1:30 (*filled diamond*), 1:200 (*filled triangle*) [Ru] = 10 μM, $[Fe(CN)_6]^{4-}$ = 0.1 M

$$I_0/I = 1 + k_{sv}[Q] \quad (2)$$

where I_0 and I are the fluorescence intensities in the absence and presence of quenching $[Fe(CN)_6]^{4-}$. K_{sv} is the linear Stern–Volmer constant and $[Q]$ is the quencher concentration. In the plot of I_0/I versus $[Q]$ slope is the K_{sv} in Fig. 4. The K_{sv} values for the complexes in the absence of DNA and in the presence of DNA are given in Table 3. The K_{sv} values are smaller in presence of DNA as explained by repulsions of the highly negative $[Fe(CN)_6]^{4-}$ from the DNA polyanion backbone which hinders access of $[Fe(CN)_6]^{4-}$ to the DNA bound complexes [39, 40], hence quenching is small. At higher concentration of DNA the slope is almost zero indicating that the bound species is inaccessible to quencher. From absorption and fluorescence spectroscopy studies the binding of complexes with DNA is in the order **1** > **2** > **3** > **4**.

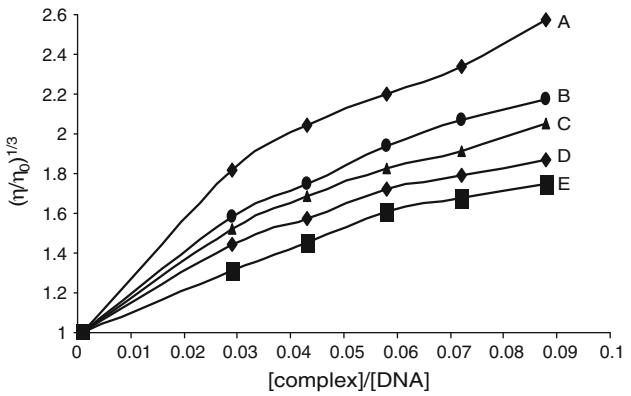

Fig. 5 Effect of increasing amounts of ethidium bromide (**A**), complex **1** (**B**), complex **2** (**C**), complex **3** (**D**) and complex **4** (**E**) on the relative viscosity of calf thymus DNA at 30 (±0.1) °C. [DNA] = 0.5 mM

Viscosity measurements

The viscosity studies provide a strong evidence for intercalation or groove binding [41]. A classical intercalation model demands that the DNA helix must lengthen as base pairs are separated to accommodate the binding ligand, leading to increase of DNA viscosity. In contrast, a partial intercalation could bend the DNA helix and reduce its effective length and, concomitantly, its viscosity [27, 42]. The effect of complexes **1**, **2**, **3** and **4** on the viscosity of rod-like DNA are shown in Fig. 5. For complexes **1** and **2** upon increasing the amount of complex, the viscosity of DNA increases steadily, while for the complexes **3** and **4** the increase in viscosity is comparatively less. Ethidium bromide is a known DNA classical intercalator and increases the relative specific viscosity by lengthening of the DNA double helix through the intercalation mode. The increased degree of viscosity, which may depend on the intercalative affinity of complex, and follows the order EB > **1**>**2** > **3**>**4**.

Thermal denaturation studies

According to the literature [43, 44], the intercalation of natural or synthesized organics and metallointercalators generally results in a considerable increase in melting temperature (T_m). As intercalation of the complexes into DNA base pairs causes stabilization of base stacking and hence raises the melting temperature of the double-stranded DNA. The DNA melting experiment is useful in establishing the extent of intercalation [35] of the complex with DNA. The complexes were incubated with CT–DNA and their temperature raised from 25 to 80 °C and the OD at 260 nm was monitored [45]. Here T_m of CT–DNA was found to be 60.8 °C in tris-buffer, with addition of the complex (10 μL) to DNA, T_m increases dramatically to 73.9 ± 0.2, 72.3 ± 0.2, 69.6 ± 0.2 and 68.3 ± 0.2 °C,

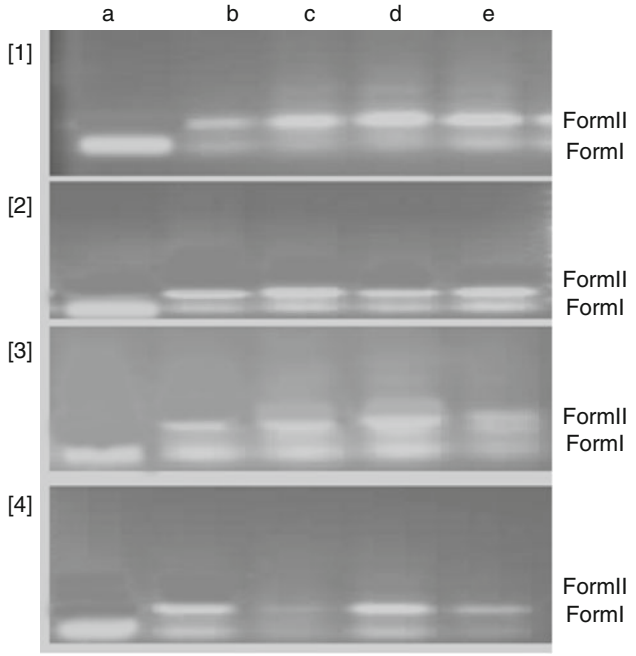

Fig. 6 Photocleavage studies of pBR322 DNA, in the absence and presence of complexes $[Ru(phen)_2fyip]^{2+}$ [1], $[Co(phen)_2fyip]^{3+}$ [2], $[Ru(bpy)_2fyip]^{2+}$ [3] and $[Co(bpy)_2fyip]^{3+}$ [4] light after 30 min irradiation at 302 nm. *Lane a* control plasmid DNA (untreated pBR322), *lane b–e* addition of complexes in amounts of 10, 20, 30, 40 μL

respectively. These results also suggest the interaction of complex **1** with DNA is more among the three complexes.

DNA photocleavage

The sequence-specific cleaving agent is a new cleaving agent composed of DNA recognizing system and cleaving system. They can cleave DNA in any sequence. The octahedral transition metal complex is stable to the oxidant, but sensitive to light. Upon irradiation, they can cleave DNA by generating singlet oxygen, or hydroxyl radical. The features common to these complexes are that these complexes have high affinity for double-strand DNA and they can intercalate into the base pairs of DNA. The plasmid DNA exits in three different forms; that is super coiled, nicked and linear. These different types can be distinguished by electrophoresis, since they migrate in different velocity, as super coiled type DNA migrates the quickest, and nicked type DNA is the slowest and linear is in between. Figure 6 shows the gel electrophoresis separation of pBR322 DNA after incubated with Ru(II) and Co(III) complexes (**1**–**4**) and irradiation at 302 nm. No DNA cleavage was observed for the control in which metal complex was absent (lane a) with increase in the concentration of the complex, the amount of form I of plasmid

Table 4 Antibacterial activity of four complexes with standard antibiotics

S. no.	Name of the compound	*Staphylococcus aureus* (mm)	*Klebsiella* (mm)	*Pseudomonas* (mm)	*E. coli* (mm)
1	DMSO	No inhibition	No inhibition	No inhibition	No inhibition
2	Compound I	20	18	11	17
3	Compound II	8	8	No inhibition	13
4	Compound III	7	No inhibition	No inhibition	No inhibition
5	Compound IV	10	No inhibition	No inhibition	No inhibition
6	Ampicillin	28	25	No inhibition	18
7	Co-trimaxizole	24	23	No inhibition	23
8	Norfloxacin	20	17	22	28

Table 5 Detection of minimum inhibitory concentration of complexes and standard antibiotics

S. no.	Name of the compound	MIC (mcg)	*Staphylococcus aureus* (mcg)	*Klebsiella* (mcg)	*Pseudomonas* (mcg)	*E. coli* (mcg)
1	Compound I	20	20	25	20	20
2	Compound II	50	50	50	Nil	30
3	Compound III	60	60	Nil	Nil	Nil
4	Compound IV	40	40	Nil	Nil	Nil
5	Ampicillin	10	10	10	10	10
6	Co-trimaxizole	1.25	1.25	1.25	Nil	1.25
7	Norfloxacin	10	10	10	10	10

DNA diminishes gradually, where as form II increases [15, 46]. All complexes exhibit plasmid DNA cleavage.

Antibacterial activities

Zone of inhibition was measured for four complexes as well as standard antibiotics and the results are given in Table 4. The complexes **1** and **2** are very promising in exhibiting their ability to inhibit/destroy both Gram positive and Gram negative pathogenic bacteria. Whereas compounds **3** and **4** have shown antibacterial activity only on Gram positive bacteria. The MIC is the lowest concentration of a drug that inhibits more than 99% of the population. Complexation reduces the polarity of the metal ion because of the partial sharing of its positive charge with the donor groups. Chelation makes the chelating ligand more potent bactereostatic agents thus inhibiting the growth of bacteria more than the chelating ligands. Such complexation could enhance the lipophilic character of the central metal ion, which subsequently favours permeation through the lipid layers of cell membrane [47]. For complex **1** the MIC is 20 μg for Gram positive bacteria and 25 μg for Gram negative bacteria. For complex **2** MICs 50 μg for both Gram positive and Gram negative bacteria, for complex **3** and **4** MIC is 60 and 40 μg against Gram positive bacteria. The MIC data of four complexes are given in Table 5. So the antimicrobial activity of four complexes is in the order of **1** > **2** > **3** > **4**. The low MIC indicates that they can be used as therapeutic agents after studying their selective toxicity and other necessary tests.

Conclusions

The results described in this study demonstrate that extension of planarity of ligand can bind strongly and can intercalate into the base pairs of DNA. The planarity of the modified 1,10-phenanthroline ligands plays an important role in dictating the DNA binding affinity. Absorption, emission, thermal denaturation studies tells that, these complexes can intercalate into DNA base pairs via fyip ligand. DNA-binding constants of the Ru(II) or Co(III) complexes with phenanthroline as ancillary ligand are large as compared to bipyridyl as ancillary ligand. This support the role of ancillary ligand, when intercalating is same the binding strength depends on the planarity of the ancillary ligands. The DNA photocleavage abilities of these complexes follow the order **1** < **2** < **3** < **4**.

References

1. Zeglis, B.M., Pierre, V.C., Barton, JK.: Metallo-intercalators and metallo-insertors. Chem. Commun. 4567–4579 (2007)
2. Schuster, G.B., Landman, U.: The mechanism of long-distance radical cation transport in duplex DNA ion-gated hopping of polaron-like distortions. Top. Curr. Chem. **236**, 139–161 (2004)
3. Elias, B., Kirsch-De Mesmaeker, A.: Photo-reduction of poly-azaaromatic Ru(II) complexes by biomolecules and possible applications. Coord. Chem. Rev. **250**(13–14), 1627–1641 (2006)
4. Gao, F., Chao, H., Ji, L.N.: DNA binding, photocleavage, and topoisomerase inhibition of functionalized ruthenium(II)-polypyridine complexes. Chem. Biodivers. **5**, 1962–1979 (2008)
5. Gratzel, M. (ed.): Energy Resources Through Photochemistry and Catalysis. Academic Press, New York (1983)
6. Creutz, C., Sutin, N.: Reaction of tris(bipyridine)ruthenium(III) with hydroxide and its application in a solar energy storage system. Proc. Natl Acad. Sci. **72**, 2858–2862 (1975)
7. Lin, C.T., Sutin, N.: Quenching of the luminescence of the tris(2,2′-bipyridine) complexes of ruthenium(II) and osmium(II). Kinetic considerations and photogalvanic effects. J. Phys. Chem. **80**(2), 97–105 (1976)
8. Kumar, C.V., Barton, J.K., Turro, N.J.: Photo physics of ruthenium complexes bound to double helical DNA. J. Am. Chem. Soc. **107**, 5518–5523 (1985)
9. Meyer, T.J.: Photochemistry of metal coordination complexes: metal to ligand charge transfer excited states. Pure Appl. Chem. **58**, 1193–1200 (1986)
10. Purugganan, M.D., Kumar, C.V., Turro, N.J., Barton, J.K.: Accelerated electron transfer between metal complexes mediated by DNA. Science **241**, 1645–1649 (1988)
11. Boerner, L.J.K., Zaleski, J.M.: Metal complex–DNA interactions: from transcription inhibition to photoactivated cleavage. Curr. Opin. Chem. Biol. **9**, 135–144 (2005)
12. Clarke, M.J.: Erratum to ruthenium metallopharmaceuticals. Coord. Chem. Rev. **232**, 69–93 (2002)
13. Ji, L.-N., Zou, X.-H., Liu, J.-G.: Shape- and enantioselective interaction of Ru(II)/Co(III) polypyridyl complexes with DNA. Coord. Chem. Rev. **216–217**, 513–536 (2001)
14. Erkkila, K.E., Odom, D.T., Barton, J.K.: Recognition and reaction of metallointercalators with DNA. Chem. Rev. **99**, 2777–2795 (1999)
15. Zhang, Q.-L., Liu, J.-G., Chao, H., Xue, G.-Q., Ji, L.-N.: DNA-binding and photocleavage studies of cobalt(III) polypyridyl complexes: $[Co(phen)_2IP]^{3+}$ and $[Co(phen)_2PIP]^{3+}$. J. Inorg. Biochem. **83**, 49–55 (2001)
16. Zhang, Q.-L., Liu, J.-G., Liu, J.-Z., Li, H., Yang, Y., Xu, H., Chao, H., Ji, L.-N.: Effect of intramolecular hydrogen-bond on the DNA-binding and photocleavage properties of polypyridyl cobalt(III) complexes. Inorg. Chim. Acta **339**, 34–40 (2002)
17. Zhang, Q.-L., Liu, J.-G., Liu, J., Xue, G.-Q., Li, H., Liu, J.-Z., Zhou, H., Qu, L.-H., Ji, L.-N.: DNA-binding and photocleavage studies of cobalt(III) mixed-polypyridyl complexes containing 2-(2-chloro-5-nitrophenyl)1-H-imidazo[4,5-f][1,10 phenanthroline]. J. Inorg. Bio Chem. **85**(4), 291–296 (2001)
18. Zhang, Q.-L., Liu, J.-G., Xu, H., Li, H., Liu, J.-Z., Zhou, H., Qu, L.-H., Ji, L.-N.: Synthesis, characterization and DNA-binding studies of cobalt(III) polypyridyl complexes. Polyhedron **20**, 3049–3055 (2001)
19. Zhang, Q.-L., Liu, J.-H., Ren, X.-Z., Xu, H., Huang, Y., Liu, J.-Z., Ji, L.-N.: A functionalized cobalt(III) mixed-polypyridyl complex as a newly designed DNA molecular light switch. Inorg. Biochem. **95**, 194–198 (2003)
20. He, X.F., Wang, L., Ji, L.N., et al.: Characterization and DNA binding study of Co(III) polypyridyl mixed-ligand complexes. Polyhedron **17**(18), 3161–3166 (1998)
21. Shilpa, M., Nagababu, P., Satyanarayana, S.: Studies on DNA-binding and plasmid-cleavage of cobalt (III) mixed ligand complexes. Main Group Chem. **8**, 33–45 (2009)

22. Nagababu, P., Shilpa, M., Satyanarayana, S., Naveena Lavanya Latha, J., Karthikeyan, K.S., Rajesh, M.: Interaction of cobalt(III) polypyridyl complexes containing asymmetric ligands with DNA. Transit. Met. Chem. **33**, 1027–1033 (2008)
23. Marmur, J.: A procedure for isolation of deoxyribonucleic acid from microorganism. J. Mol. Biol. **3**, 208–214 (1961)
24. Reichmann, M.E., Rice, S.A., Thomas, C.A., Doty, P.: A further examination of the molecular weight and size of desoxypentose nucleic acid. J. Am. Chem. Soc. **76**, 3047–3053 (1954)
25. Wolfe, A., Shimer, G.H., Meehan, T.: Polycyclic aromatic hydrocarbons physically intercalate into duplex regions of denatured DNA. Biochemistry **26**, 6392–6396 (1987)
26. Chaires, J.B., Dattagupta, N., Crothers, D.M.: self association of daunomycin. Biochemistry **21**(17), 3927–3932 (1982)
27. Satyanarayana, S., Dabrowiak, J.C., Chaires, J.B.: Tris(phenanathroline) ruthenium(II) enantiomer interactions with DNA: mode and specificity of binding. Biochemistry **32**, 2573–2584 (1993)
28. Drew, W.L., Barry, A.L., Toole, R.O., Shreeis, J.C.: Reliability of the Kirby-Bauer Disc diffusion method for detecting methicillin-resistant strains of *Staphylococcus aureus*. Appl. Microbiol. Am. Soc. Microbiol. **24**, 240 (1972)
29. Yamada, M., Tanaka, Y., Yoshimato, Y., Kuroda, S., Shimao, I.: Synthesis and properties of diamino-substituted dipyrido [3,2-a: 20, 30-c] phenazine. J. Bull. Chem. Soc. Jpn. **65**, 1006–1011 (1992)
30. Sullivan, B.P., Salmon, D.J., Meyer, T.J.: Mixed phosphine 2,2′-bipyridine complexes of ruthenium. Inorg. Chem. **17**, 3334–3341 (1978)
31. Vlcek, A.A.: Preparation of $Co(dipy)_2X^{2+}$ complexes (X− = chloride, bromide, iodide, nitrite) by controlled oxidative processes. Inorg. Chem. **6**, 1425–1427 (1967)
32. Steck, E.A., Day, A.R.: Reactions of phenanthraquinone and retenequinone with aldehydes and ammonium acetate in acetic Acid solution. J. Am. Chem. Soc. **65**, 452–456 (1943)
33. Barton, J.K., Danishefsky, A.T., Goldberg, J.M.: Tris(phenanthroline)ruthenium(II): stereoselectivity in binding to DNA. J. Am. Chem. Soc. **106**, 2172–2176 (1984)
34. Tysoe, S.A., Morgan, R.J., Baker, A.D., Strelkas, T.C.: Spectroscopic investigation of differential binding modes of .DELTA.- and .LAMBDA.-Ru(bpy)2(ppz)2+ with calf thymus DNA. J. Phys. Chem. **97**, 1707–1711 (1993)
35. Kelly, T.M., Tossi, A.B., McConnell, D.J., OhUigin, C.: A study of the interactions of some polypyridylruthenium (II) complexes with DNA using fluorescence spectroscopy, topoisomerisation and thermal denaturation. Nucleic Acids Res. **13**, 6017–6034 (1985)
36. Wu, J.-Z., Li, L., Zen, T.-X., Ji, L.N.: Synthesis, characterization and luminescent DNA-binding study of a series of ruthenium complexes containing 2-arylimidazo[f]1,10-phenanthroline. Polyhedron **16**, 103–107 (1997)
37. Pyle, A.M., Rehmann, J.P., Meshoyrer, R., Kumar, C.V., Turro, N.J., Barton, J.K.: Mixed-ligand complexes of ruthenium(II): factors governing binding to DNA. J. Am. Chem. Soc. **111**, 3051–3058 (1989)
38. Joseph, R., Lakowicz, G.W.: Quenching of fluorescence by oxygen. Probe for structural fluctuations in macromolecules. Biochemistry **12**, 4161–4170 (1973)
39. Lakowicz, J.R.: Principles of Fluorescence Spectroscopy. Plenum Press, New York (1983)
40. Kumar, C.V., Turro, N.J., Barton, J.K.: Photophysics of ruthenium complexes bound to double helical DNA. J. Am. Chem. Soc. **107**, 9319–9324 (1985)
41. Sigma, D.S., Mazumder, A., Perrin, D.M.: Chemical nucleases. Chem. Rev. **93**, 2295–2316 (1993)
42. Satyanarayana, S., Dabrowiak, J.C., Chaires, J.B.: Neither D- nor L-tris (phenanathroline) ruthenium (II) binds to DNA by classical intercalation. Biochemistry **31**, 9319–9324 (1992)
43. Waring, M.J.: Complex formation between ethidium bromide and nucleic acids. J. Mol. Biol. **13**, 269–282 (1965)
44. Neyhart, G.A., Grover, N., Smith, S.R., Kalsbeck, W.A., Fairly, T.A., Cory, M., Thorp, H.H.: Binding and kinetics studies of oxidation of DNA by oxoruthenium(IV). J. Am. Chem. Soc. **115**, 4423–4428 (1993)
45. Tselepi-Kalouli, E., Katsaros, N.: The interaction of $[Ru(NH_3)_5Cl]^{2+}$ and $[Ru(NH_3)_6]^{3+}$ ions with DNA. J. Inorg. Biochem. **37**, 271–282 (1989)
46. Jin, L., Yang, P.: Synthesis and studied of Co(III) mixed-ligand complex containing dipyrido[3, 2-a-c] phenazine and phen. Polyhedron **16**, 3395–3398 (1997)
47. Tweedy, B.G.: Phytopathology, **55**, 910 (1964)